Hybrid (Symbolic-Numerical) Optimization in Mechanism Design for the Elimination of Redundant Constraints

D. A. Hoeltzel
Associate Professor.

Wei-Hua Chieng
Graduate Research Assistant.

Laboratory for Intelligent Design,
Department of Mechanical Engineering,
Columbia University,
New York, New York 10027

Hybrid optimization, a new approach to design optimization employing both symbolic reasoning and algorithmic analysis, has been applied to the design of kinematic pairs in mechanisms. This hybrid design methodology provides a three-step systematic approach for (1) combining the degrees-of-freedom found in simple, lower kinematic pairs to obtain more complex but robust higher pairs, (2) judging inappropriately assigned joints for the elimination of redundant kinematic constraints and harmful mobilities, and (3) assisting nonexpert designers in applying nonlinear programming algorithms for detailed numerical design optimization of kinematic pairs. An example taken from the design of a spatial mechanism, specifically a universal joint, is presented and serves to demonstrate the utility of this procedure for detailed hybrid design optimization of kinematic pairs in mechanisms.

Introduction

Today, one of the challenges of computer-based optimization lies in the application of artificial intelligence (AI) principles to the creation of systematic and well-structured design procedures [4], thereby eliminating the typical ad hoc approach to design. When numerical and symbolic computational techniques are in some way coupled, the resulting program may be classified as a hybrid system [10]. Hybrid system approaches are typically found in engineering analysis applications where an expert system is required to set up the data which defines the problem, execute the analysis programs and retrieve the output results for subsequent evaluation. Design optimization problems are well-suited for formulation as hybrid problems. For example, Chieng and Hoeltzel [2], introduced the concept of a hybrid (symbolic-numerical) optimization framework utilizing a *metacell* approach for the near optimal design of mechanical components. Their framework contained, among other cells, a *systolic* optimization design cell representing a terse *knowledge base* of sufficient domain (mechanical design) knowledge as well as characteristics of design equations for mechanical components which are used to control the numerical part of the hybrid optimization process. This systematic approach has been employed in the design of a universal joint and can be extended to the design of other mechanisms and mechanical components as well [9].

Universal joints are used extensively to couple misaligned power shafts. Mazziotti [14] presents a discussion of some of the more important types of universal joints emphasizing the rugged construction, low cost, of serviceability and other advantageous features associated with the cross and yoke type universal joint. Several investigators [1, 11, 19, 25, 34] have performed analyses on this type of universal joint. However, nowhere in the literature is it possible to find information related specifically to the optimum kinematic and geometric design of universal joints.

The concept of elimination of *redundant kinematic constraints and harmful mobilities* has been incorporated and automated in an approach to mechanism design referred to by Reshetov [21, 22] as the rational design of *self-aligning mechanisms*. In an earlier and more basic work, Whitehead [32] discusses a similar concept called precision kinematic design and applies it to the design of accurate mechanisms in precision instruments.

The primary objective of this study is the determination of the optimal design of the pin-yoke connection and the subsequent optimization of the entire universal joint based on static, kinematic and dynamic fatigue design criteria using a hybrid design approach.

Description of the Kinematic Model

The kinematic model used to represent the universal joint is the spatial four bar mechanism (Fig. 1). The mechanism contains six turning pairs with intersecting axes OA_1, OA_2, OA_3, and OA_4. The link dimensions can be identified in terms of great circular arcs $A_1A_2A_5$, $A_3A_4A_6$ and one normal crossed bar having four ends denoted by A_2, A_3, A_5, and A_6. The angle between the input shaft and the output shaft is denoted by β,

Note: *Italicized* words and phrases are defined in the glossary, alphabetically.

Contributed by the Mechanisms Committee for publication in the JOURNAL OF MECHANICAL DESIGN. Manuscript received January 1988.

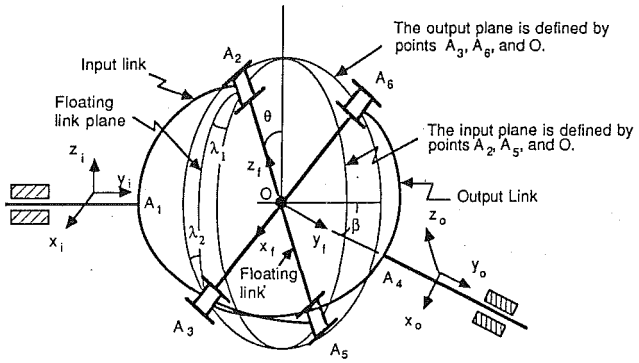

Fig. 1 Kinematic skeleton diagram of the general cross and yoke type universal joint

where $\beta > 0$. Subject to applications without high speed and load, as with small mechanical component design, the cross and yoke type universal joint yields the smallest possible design [1]. However, in heavy load or high speed applications, modifications to the design of this joint will be shown to produce improvements in, and under ideal conditions eliminate, the reaction forces acting on the input and output shafts.

The general strategy followed in this paper for the optimum design of the universal joint proceeds through kinematic, static, and dynamic fatigue analyses, incorporating symbolic and algorithmic optimization procedures.

Kinematic Synthesis

Under this rubric, general universal joint design procedures [29] are reviewed, followed by a discussion of the hybrid optimal design procedure.

The generalized Chebychev-Gruebler mobility criterion (general degree-of-freedom equation), using Freudenstein's notation [6], may be expressed as:

$$A = \sum_{i=1}^{j} f_i = F - \lambda(\ell - j - 1) \tag{1}$$

where the number of independent circuits or closed loops is given by,

$$L_{ind} = (A - 1)/\lambda \tag{2}$$

Table 1 Kinematic pairs with uncoupled degrees-of-freedom

Degrees of Freedom	Kinematic Pairs	Schematic Representation†
One	Revolute (R), Prismatic (P)‡	
Two	Slotted spheric (SlS), Torus (T), Cylinder (Cy)‡, Roller in Slot (RS)	
Three	Spheric (S), Sphere slotted (SS)‡, Plane (Pl)	
Four	Sphere groove (SG)‡, Sphere cylinder pair (SCP), Cylinder plane pair (CPP)	
Five	Sphere plane (SP)‡	

For the universal joint, $F = 1$, $\lambda = 6$ (spatial), $\ell = 4$, and $j = 6$. Based on these values, equation (1) yields a value of $A = 19$ dof and, substituting this numerical value for A into equation (2) yields a value of $L_{ind} = 3$ closed loops. This is in agreement with the schematic diagram in Fig. 1, where the three loops are given by A_2-A_1-A_5, A_3-A_4-A_6, and A_1-ground-A_4.

Yang [33] determined that the classical cross and yoke type universal joint has three indeterminate unknowns. Based on experimental results, Fischer [5] was able to confirm the existence of axial forces acting on the pins which connect the cross to the yoke for a specific type of universal joint [3]. From a physical standpoint, these redundant indeterminants have the potential to increase internal forces and moments which may cause unpredictable wear or damage to the structure of the universal joint. Upon closer examination of the cross and yoke type universal joint it can be seen that the indeterminants have arisen due to the inability of the designer to recognize the importance of their elimination to the design. Subject to the goal of the elimination of redundant kinematic constraints, a symbolic optimization procedure has been developed.

Symbolic Optimization

A symbolic optimization program knowledge base has been

Nomenclature

Universal joint schematic symbols (see Fig. 1):

- O = origin of the universal joint
- A_1 = input shaft bearing, A_4 = output shaft bearing
- A_2, A_3, A_5, A_6 = intermediate joints
- λ_1 = intersection angle between floating link plane and input link plane
- λ_2 = intersection angle between floating link plane and output link plane
- β = shaft misalignment angle
- θ = input shaft angle

Ball-Pin type universal joint dimensions (see Fig. 10):

- α = angle defining the spherical contact area at the ball-yoke connection
- L = length of floating block
- R_p = radius of pins on cylinder ends
- R_b = radius of pins on ball ends
- L_p = insertion length of pin plug in floating link
- t = thickness of yoke
- W = width of yoke
- H_1 = extended tip portion of yoke
- H_2 = root portion of yoke
- d = distance between yoke and floating block
- R = radius of input and output shafts

Chebychev-Gruebler mobility criterion (general degree of freedom equation):

- A = total degrees of freedom (dof) of the joints and bearings
- F = number of degrees of freedom (mobility) of the complete mechanism
- ℓ = number of links, including the fixed link

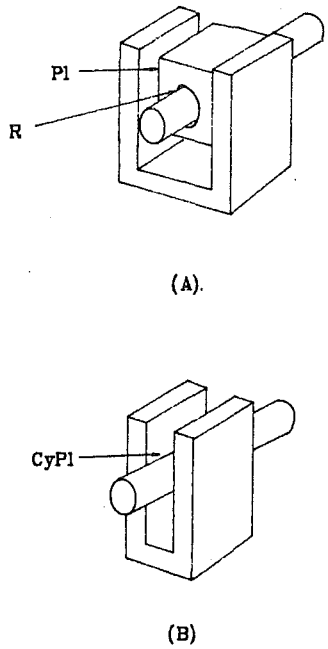

Fig. 2 Combining a revolute joint (*R*) with a plane pair (*Pl*) to yield a composite joint with surface contact that is kinematically equivalent to the cylinder plane pair (*CyPl*)

developed for (1) combining degrees-of-freedom of lower kinematic pairs into higher pairs to increase the durability and load transfer capability of kinematic joints and for (2) eliminating redundant kinematic constraints and harmful mobilities in mechanism design.

Based on a compilation of degree-of-freedom assignments for kinematic pairs [6, 28] as shown in Table 1, and on the work by Reshetov [20] and others [21, 26] on the enumeration of *kinematic connections* described in Appendix I, a systematic methodology for combining the degrees-of-freedom of lower kinematic pairs into higher pairs for the creation of robust kinematic connections has been developed as one portion of the symbolic part of the hybrid optimization process. As an example, summation of the degrees-of-freedom of a revolute pair (R) with a plane pair ($P1$), each having area contact, produces a composite joint kinematically equivalent to that of a cylinder plane pair (CyP), which only possesses line contact, in accordance with the applied external boundary constraints (Fig. 2).

Many kinematic pairs having more than three degrees-of-freedom provide line or point contact. In order to increase joint contact area and thereby increase the load carrying capacity of a mechanism (requiring joints with more than three degrees-of-freedom), composite joints (kinematic connections) which combine lower degree-of-freedom kinematic pairs into higher degree-of-freedom pairs, have been systematically enumerated. This technique has been used to generate pairs containing three, four, and five degrees-of-freedom, respectively, as shown schematically in Table 2.

In addition, the technique possesses utility beyond that for fabricating more robust kinematic connections. It is also possible to transfer certain combinations of forces and moments which single kinematic pairs are unable to transfer. For example, only with the appropriate combination of cylinder pairs is it possible to transmit a torque and a force simultaneously along the same axis, as demonstrated by the kinematic connection shown in Fig. 3(*a*). Other examples of this have been noted in Table 2 as theoretical higher pairs which do not exist as single kinematic pairs.

Combining lower pairs to obtain higher pairs may not always be feasible from a practical standpoint; however, since in certain cases the composite kinematic connection may become particularly awkward if not impossible to manufacture and operate effectively. The series combination of three prismatic pairs for transmitting torques about three orthogonal axes without simultaneously transmitting any forces, as shown in Fig. 3(*b*), is a representative example of this problem. Although this connection is particularly cumbersome it does find limited application in the design of interconnections for crossheads and ways for machine tools.

A heuristic approach for judging inappropriately assigned joints, i.e, those possessing redundant constraints, has also been developed. In order to eliminate redundant kinematic constraints within given mechanisms it is first necessary to systematically enumerate them, that is; determine (*1*) how many there are, (*2*) which pairs contain them, and (*3*) precisely which constraints (θ_x, θ_y, θ_z, x, y, z) are redundant within each of the pairs. Once the existence and location of these constraints have been enumerated, lower pairs and kinematic connections devoid of such constraints can be substituted.

Nomenclature (cont.)

j = number of joints and bearings (assumed binary, i.e., connecting two links)
λ = degree of freedom of the space within which the mechanism operates
f_i = degree of freedom of joint i
L_{ind} = number of closed loops in the mechanism

Modified Malyshev and Ozol redundant constraint equations:

p_i = number of pairs having i constraints or ($\lambda - i$) mobilities

Additional Symbols:

F_{ij} = force acting along the ith coordinate direction, on the jth joint
M_{ij} = moment acting about the ith coordinate direction, on the jth joint where $j = 1,2,3 \langle -- \rangle x, y, z$ $j = 1,2,3,4,5,6$
T_{in}, T_{out} = torque applied to the input shaft and output shaft, respectively
E = material elastic constant
K_b = stress concentration factor in bending
ν = Poisson's ratio
K_y = stress concentration factor in yielding
$(\sigma_s)_{max}$ = maximum surface fatigue stress
$(\sigma_b)_{max}$ = maximum bending fatigue stress
$(\sigma_t)_{max}$ = maximum tensile fatigue stress
$(\sigma_{rs})_{max}$ = maximum radial normal stress (spherical surface contact)
$(\sigma_{rc})_{max}$ = maximum radial normal stress (cylindrical surface contact)

Table 2 Combination of lower pairs to obtain series kinematic connections for higher pairs

Total degrees-of-freedom	D.O.F.A.	Theoretical higher pair	Combination of lower pairs	D.O.F.A.	Theoretical higher pair	Combination of lower pairs	D.O.F.A.	Theoretical higher pair	Combination of lower pairs
5	T^2 R^3		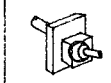	T^3 R^2	Does not exist.	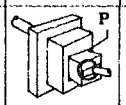			
4	T^1 R^3	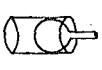	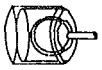	T^2 R^2 (I)			T^2 R^2 (II)		
	T^2 R^2 (III)	Does not exist.		T^3 R^1	Does not exist.				
3	R^3			T^1 R^2 (I)	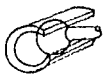		T^1 R^2 (II)	Does not exist.	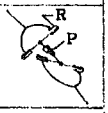
	T^2 R^1 (I)			T^2 R^1 (II)	Does not exist.		T^3	Does not exist.	

D.O.F.A.: degree-of-freedom assignment T: translation R: rotation

A. P. Malyshev [13] developed an expression for the mobility of a mechanism in terms of the number of redundant constraints it possesses. This expression has been generalized in accordance with the notation used by Freudenstein [6] in equation (1). In a mechanism containing a total of ℓ links ($\ell - 1$ of which are movable) and q redundant constraints, operating in a space having λ degrees of freedom, and with p_i pairs each of which imposes i constraints (permits $\lambda - i$ mobilities) between the links it connects.

$$F=\lambda(\ell-1)-\left(\sum_{i=1}^{\lambda-1} ip_i-q\right) \tag{3}$$

Solving equation (3) for the number of redundant constraints yields

$$q=F-\lambda(\ell-1)+\sum_{i=1}^{\lambda-1} ip_i \tag{4a}$$

Expanding the last term in equation (4*a*) for clarity yields an expression for the number of redundant constraints:

$$q=F-\lambda(\ell-1)+(\lambda-1)p_{\lambda-1}+(\lambda-2)p_{\lambda-2} +\ldots+3p_3+2p_2+p_1 \tag{4b}$$

Another structural formula for calculating the number of redundant constraints within a given mechanism has been developed by O. G. Ozol [17] in terms of the mobility, F, the number of *independent loops*, L_{ind} [which may be obtained from equation (2)] and the sum of the mobilities of the kinematic pairs, $\sum_{i=1}^{\lambda-1}(\lambda - i)p_i$, which comprise the mechanism. The original formulation as developed by Ozol has been generalized in accordance with the notation used by Freudenstein [6], and can be expressed in a compact form as:

$$q=F+\lambda L_{ind}-\sum_{i=1}^{\lambda-1}(\lambda-i)p_i \tag{5a}$$

or in expanded form, for clarity, this can be rewritten as

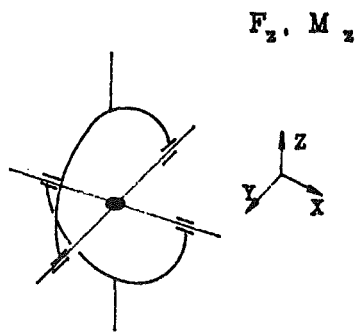

Fig. 3(*a*) Kinematic connection for transmitting a torque and a force along the same axis from the series combination of cylindrical joints

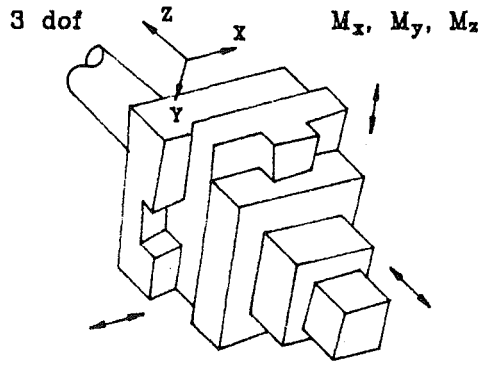

Fig. 3(*b*) Example of an awkward kinematic connection

$$q=F+\lambda L_{ind}-(\lambda-(\lambda-1))p_{\lambda-1}-(\lambda-(\lambda-2))p_{\lambda-2} -\ldots-3p_3-4p_2-5p_1 \tag{5b}$$

It is important to note that neither equation (4*a*) nor equation (5*a*) can provide a unique solution to the problem of eliminating redundant constraints or harmful mobilities. These equations are simply an analytical method for determining their number, hence the need for a heuristic approach for their elimination.

A sample of some of the rules for judging the existence of redundant constraints and for making suggestions concerning

how redundant constraints may be eliminated are listed below in the order of their generality:

Rule 1: An open loop kinematic chain contains no redundant constraints.

Rule 2: In single-loop, single mobility mechanisms and in the main loop of multiple loop mechanisms, the sum of the mobilities of the kinematic pairs equals seven if redundant constraints are absent.

Rule 3: When an independent loop comprised of two links is added to a single loop mechanism or to the main loop of a multiple loop mechanism, the sum of the mobilities of the kinematic pairs is equal to six if redundant constraints are absent.

Rule 4: Whenever possible, antifriction bearings should be utilized in order to eliminate the possibility of friction as a cause of constraint redundancy within kinematic pairs.

Rule 5: Any single closed loop in a mechanism should not contain more than two prismatic pairs, otherwise harmful (additional) mobilities will exist.

Rule 6: Two cylinder pairs should not be connected in series along parallel axes without limiting the linear mobility (i.e., travel) of one of the cylinder pairs, otherwise a harmful mobility will occur.

Rule 7: A link with a local angular (linear) mobility should have the external torque (force) about (along) the corresponding axis equal to zero, since such a torque (force) cannot be resisted.

Rule 8: A limited linear displacement requires that a force be transmitted in the kinematic pair between its links. Therefore, the notion of a limited linear displacement has as a counterpart the notion of a transmitted force.

Rule 9: A limited angular rotation requires that a torque be transmitted in the kinematic pair between its links. Therefore, the notion of a limited angular rotation has as a counterpart the notion of a transmitted torque.

Rule 10: A prismatic pair does not permit rotary mobilities, so kinematic connections should not have more than three prismatic pairs in order to avoid the existence of redundant constraints.

Rule 11: Series prismatic pairs are employed only when linear motions along orthogonal axes are required.

Rule 12: For a single loop mechanism, the presence of all three angular mobilities (θ_x, θ_y, θ_z) is necessary in order to avoid the existence of a redundant constraint.

Rule 13: Adding a new loop comprised of two pinned links, i.e, a dyad, to an existing mechanism results in a new mechanism without changing the degree-of-freedom of the mechanism. In addition, the sum of the mobilities (dof's) of its kinematic pairs equal six when there are no redundant constraints (in accordance with Rule 3).

The methodology for removing redundant constraints proceeds on a joint by joint basis and relies on an interactive dialogue between the system (through a computer program which systematically implements this methodology) and the designer. During this bidirectional dialogue the types of effort (force and/or moment and their orientation) or the types of motion (translation and/or rotation and their orientation) required to be transferred by the joint must be specified. Once the joints have been analyzed, the overall mechanism is then examined for redundant constraints and harmful mobilities. The flow of control for this process is shown in Fig. 4.

In applying this methodology to the redesign of the cross-and-yoke type universal joint, the system first calculates the number of redundant constraints (seven in this case) using equations (4*a*) or (5*a*), and then looks at each of the existing

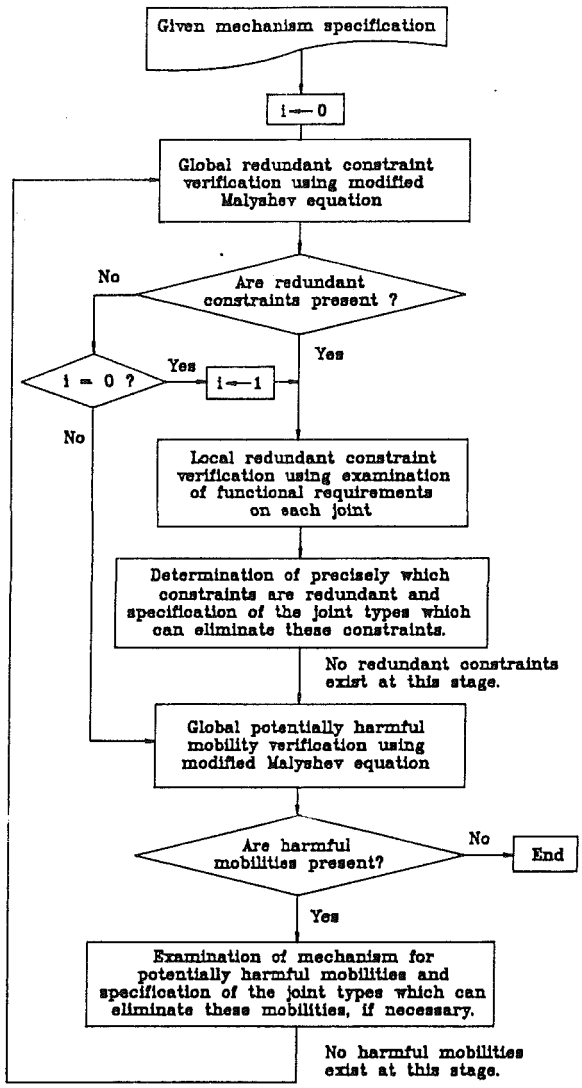

Fig. 4 Flow control for the removal of redundant constraints and potentially harmful mobilities

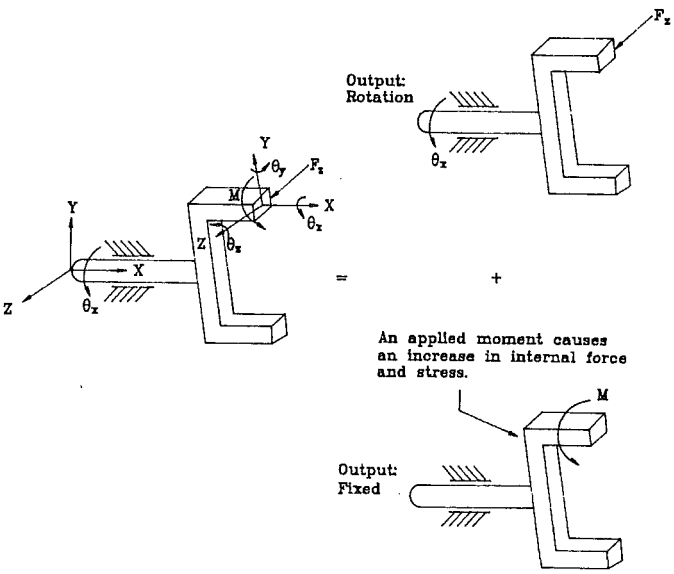

Fig. 5 For the universal joint, the effective output rotation, θ_x, should be produced only by an effective force, F_z

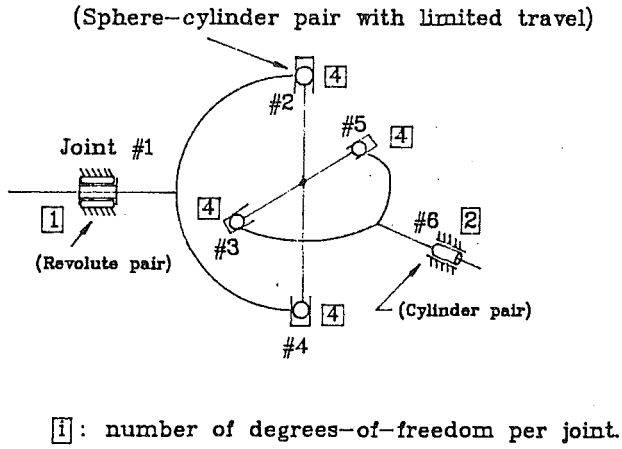

Fig. 6 Degree-of-freedom reassignment after the symbolic optimization process is completed

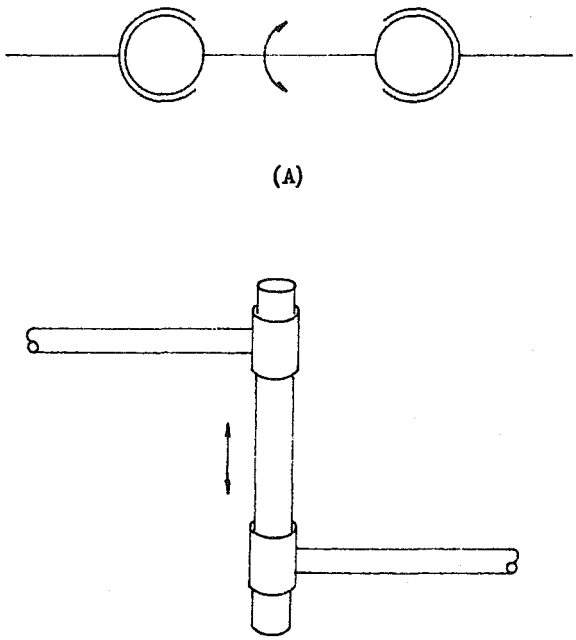

Fig. 7 Inappropriate joint assignment
(*a*) harmful rotational mobility
(*b*) harmful translational mobility

joints to determine the effort or motion required to be transferred by that joint. Arbitrarily beginning with the four intermediate joints, the designer attempts to systematically eliminate their redundant constraints by invoking the following basic principles.

Firstly, the effort or motion required to be transferred by the joint is sought. The designer notes that at each existing intermediate joint of the universal joint (Fig. 5) only a single force need be transferred across the yoke in order to transmit a torque through the universal joint, from the input shaft to the output shaft. No additional efforts are required. As currently designed, the cross-and-yoke design utilizes cylinder pairs for the intermediate joints. These joints transmit a moment in addition to a force. The ability to transmit the moment must therefore be eliminated in order to remove a redundant constraint. The possible joint types to be used to eliminate redundant constraints are enumerated from the most general (greatest number of dof's) to the least general (fewest number of dof's) type. To transfer a single force at a point with five degrees-of-freedom (most general case) calls for a *point-and-surface pair* as shown in Table 2. This pair has its degrees-of-freedom assigned as T^2, R^3. The physical embodiment of a practically usable version of this pair is the sphere-plane pair. Applying this same line of reasoning to the three remaining intermediate joints dictates the need for three additional point-and-surface pairs. Continuing this process for the remaining joints, the input joint is specified as a revolute pair while the output joint is specified as a cylinder pair. An overall total of 23 degrees-of-freedom exist after the joint reassignment process has been completed.

Recalculating the number of redundant constraints for the redesigned mechanism yields a value of -4 indicating that the overall mechanism is now underconstrained, i.e., contains potentially harmful mobilities. The designer must now consider the overall mechanism, aside from the individual joints, to determine if and where the four additional constraints may be required. In this case each of the four intermediate joints requires one additional constraint to prevent them from falling under their own weight (undergoing rigid body motion) when the mechanism rotates. These joints are then assigned as limited travel sphere-cylinder pairs (Fig. 6), each having four degrees-of-freedom (Table 2). In other less obvious cases, dynamic simulation of the mechanism may be required to determine the appropriate assignment of additional constraints to eliminate harmful mobilities.

As noted above, in the process of assigning joints in the design of a mechanism consideration must be given not only to the fulfillment of input-output requirements but also to the physical constraints required by the problem. For example, an inappropriate joint assignment may cause the output link of a mechanism to be totally undriven, Fig. 7(*a*). Figure 7(*b*) demonstrates an obvious example where inappropriate constraints have been applied to the design of a mechanism and as a result gravity can cause the intermediate link to fall under its own weight. While these represent simple examples of harmful mobilities, concepts such as this one can have significant kinematic ramifications and must therefore be given proper consideration.

For many practical applications the symbolic optimization phase of the design process can be based on a depth-first search strategy, thereby tending to produce a *local optimum*. Other applications requiring a *globally optimal* design should employ a breadth-first search strategy. Figure 8(*a*) depicts the search tree sequence and corresponding decision making logic for the appropriate assignment of degrees-of-freedom in the universal joint design, and demonstrates the breadth-first (global) nature of this "optimum" solution. Figure 8(*b*) depicts the search tree sequence for joint type assignment and demonstrates the depth-first (local) nature of this "optimum" solution.

Using the cross-and-yoke type universal joint as a starting point for the design process and systematically applying the symbolic design optimization strategies described above, a new universal joint design called the ball-pin type universal joint has been developed. Table 3 shows a comparison of the degree-of-freedom assignment for the cross-and-yoke and ball-pin universal joints.

The following steps summarize the symbolic optimization process:

(*1*) Specification of the symbolic design objective, that is the objective function and constraints which describe the optimum design objective. For the purposes of this application the objective was to minimize the redundant reactions (forces and moments) within the existing universal joint.

(*2*) Reassignment of the degrees-of-freedom on the intermediate joints to achieve the design objective. These

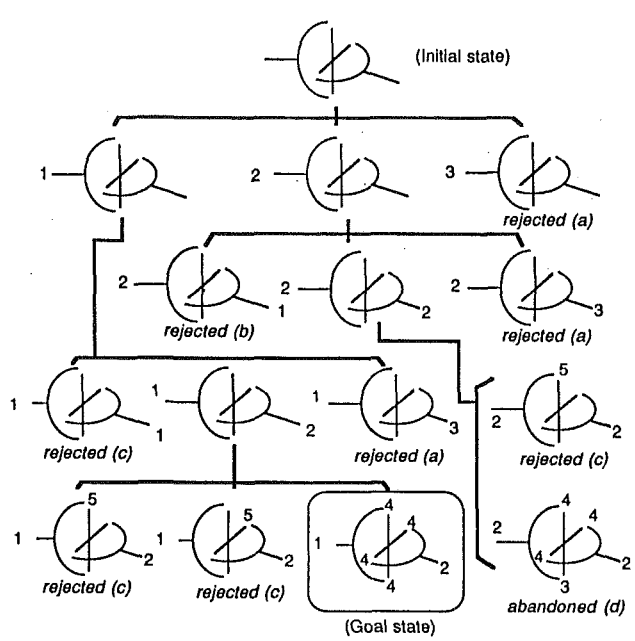

Decision making for degree-of-freedom assignment:

- Global constraint:
  General mobility equation shows that the total number of joint d.o.f. is 19

- Reasons for rejected cases:
  a. In order to adapt to practical applications, the d.o.f. of the joints on the ground link should be less than 3.
  b. Isomorphism found in the enumeration process.
  c. From a manufacturing standpoint, the joints containing more than 4 d.o.f. are difficult to fabricate (except possibly for special purposes).

- Preference for the final selection:
  d. A symmetric design is preferred in this design case.

Fig. 8(*a*) Search tree sequence for the process of degree-of-freedom assignment in the design of a universal joint

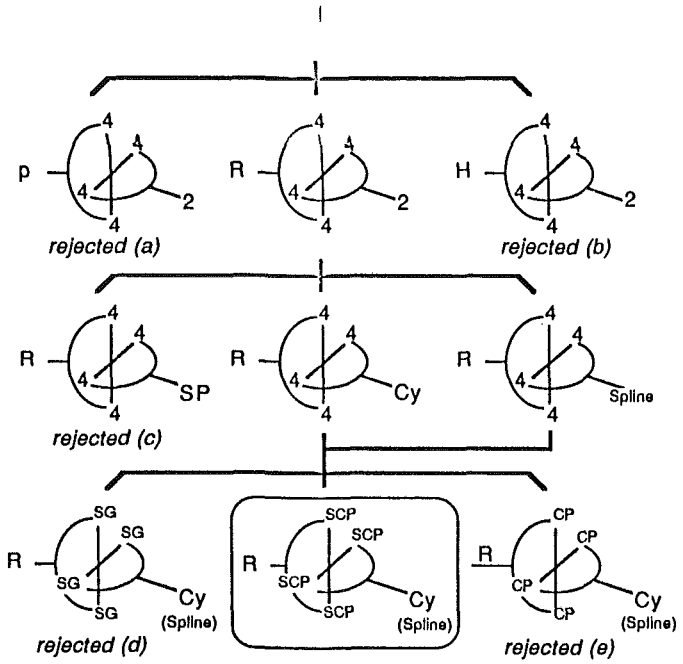

- Global constraint:
  Design is subjected to a rotary input and a rotary output

- Reasons for rejected cases:
  a. For the purpose of transmitting rotary motion, a prismatic joint is rejected.
  b. For the purpose of transmitting rotary motion, a helical joint is rejected.
  c. To prevent variation of the misalignment angle within the U-joint, the slotted spheric (SP) joint is rejected.
  d. Sphere grove (SG) joint pairs cause redundant sliding motion when misalignment angle is zero, therefore it is rejected.
  e. Cylinder plane (CP) joint failed to hold the floating link, therefore it is rejected.

Fig. 8(*b*) Search tree sequence for the process of joint type assignment in the design of a universal joint

joint assignments must also satisfy the generalized Chebychev-Gruebler mobility (general degree-of-freedom) equation.

(*3*) Refinement of the design in order to increase reliability, enhance manufacturability, and assembleability. This was implemented via the technique of combining lower kinematic pairs into higher kinematic pairs in order to increase joint contact area while maintaining kinematic equivalence.

(*4*) Comparison of the new design with the old design based on the number of redundant constraints.

Static Analysis

In applying static analysis procedures to the design of the universal joint two specific regions of the joint must be considered. The first is the input and output shaft bearings design. This was the focus of Fischer's work [5]. The other is the design of the intermediate joints. Based on the geometry depicted in Fig. 10, it is evident that the pin-yoke connection is more fragile than the input-output bearing-shaft connection and should therefore occupy the primary focus in the numerical optimization procedure.

The following coordinate systems are relevant to the analysis (Fig. 1).

(X, Y, Z): Global coordinate system corresponding to the entire universal joint.

(x_i, y_i, z_i): Coordinates corresponding to the input link. The y axis is collinear with the input shaft and the z axis is parallel to $O - A_3$.

Table 3 Kinematic comparison of cross and yoke type universal joint with ball-pin type universal joint

Kinematic factors	Cross and yoke U-joint	Ball-pin U-joint
F (number of dof)	1	1
l (number of links)	4	8
j (number of joints)	6	10
A (total number of dof of all the joints)	12	19
λ (dof of space)	6	6
q (number of redundant constraints, Eq. 4b.)	7	0

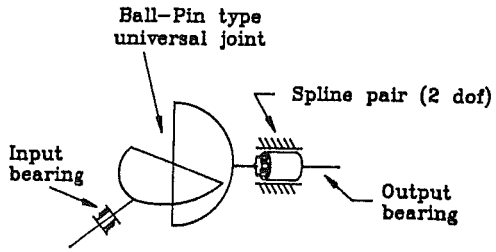

Fig. 9 Vibration acting on the input shaft is isolated across the universal joint. The oscillatory effects are absorbed by the ball-pin pairs. A spline pair has been utilized on the output shaft to remove the redundant translational force.

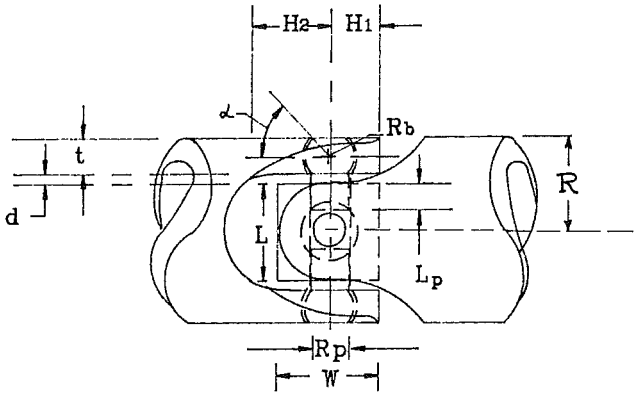

Fig. 10 Ball-pin type universal joint

(x_f, y_f, z_f): Coordinates corresponding to the floating block. The x axis is collinear with $O - A_3$ and the z axis is collinear with $O - A_2$.

(x_0, y_0, z_0): Coordinates corresponding to the output link. The x axis is parallel to $O - A_3$ and the y axis is collinear with the output shaft.

Assuming well-lubricated (frictionless) joints, and comparatively small clearances (no misalignment) between each pin and yoke, the axial forces and moments on the intermediate joints can be assumed to be zero. Based on the force and moment equilibrium equations for each link, 18 equations containing 17 unknowns (reaction forces and moments) plus one output can be solved. Using the dual number method as discussed by Yang [34], the following results have been obtained.

$$F_{i1} = F_{j1} = F_{k1} = F_{i4} = F_{j4} = F_{k4} = 0 \quad (6)$$

$$F_{j3} = F_{j6} = -F_{j5} = -F_{j2} = 0 \quad (7)$$

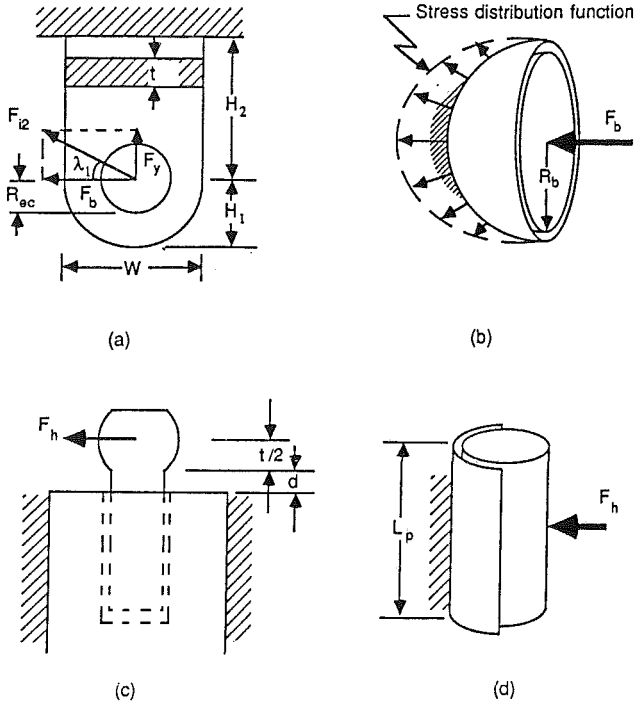

Fig. 11 Fatigue design of the yoke, block and pin
(*a*) loads acting on the yoke
(*b*) spherical contact area between ball joints and yoke assuming Hertzian contact
(*c*) loads acting on the pin
(*d*) cylindrical contact area between the pin and block

$$F_{i5} = F_{k3} = -F_{k6} = -F_{i2} = -T_{in}^{*}(\sqrt{1-\sin^2\theta\sin^2\beta}/2R\cos\beta) \quad (8)$$

While intermediate joints 2, 3, 5, and 6 are represented by the floating block coordinate systems, bearing number 1 is represented by the input shaft coordinate system and bearing number 4 is represented by the output shaft coordinate system. For example, $i2$ represents the ith coordinate of the floating block on joint number 2. The output torque is given by

$$T_{out} = M_{j4} = T_{in}^{*}(1-\sin^2\theta\sin^2\beta)/\cos\beta \quad (9)$$

The rocking torque on the input shaft is given by

$$M_{i1} = T_{in}^{*}\tan\beta\cos\theta \quad (10)$$

The rocking torque on the output shaft is given by

$$M_{k4} = -T_{in}^{*}\sin\theta\tan\beta\sqrt{1-\sin^2\theta\,\sin^2\beta} \quad (11)$$

In the above expressions, F_{ij} represents a force acting along the ith coordinate direction on the jth joint.

Based on these results the following conclusions may be drawn:

(*1*) There are no reaction forces acting on the input or output shafts.
(*2*) The reaction moments and output torque are identical to those found in the ideal case.
(*3*) Only effective forces, which generate the actual working torque (about the output shaft), exist.
(*4*) The equations of equilibrium can be directly solved without resorting to the solution of equations of deformation since the mechanism is statically determinate, thereby simplifying the design process.

Additional attractive features associated with the ball-pin type universal joint include its ability to allow greater manufacturing tolerances at the ball joint without concomitant binding of the kinematic pair as well as its ability to isolate noise and vibration from the input shaft to the output shaft and

visa versa (Fig. 9). Disadvantages associated with the ball-pin type universal joint design include increased difficulties in manufacturing and assembling of the ball joints as well as in analyzing the more complex, sphere-cylinder, intermediate joint bearings.

Fatigue Analysis

Due to the cyclic nature of the reaction forces and moments acting on the universal joint, consideration must be given to fatigue analysis. Converting the schematic diagram of the universal joint (Fig. 1) into actual design scale requires that (Fig. 10):

$$R = L/2 + d + t/2 \tag{12}$$

In order to eliminate design indeterminants, the following design decisions have been made:

(*1*) In order to reduce contact stress concentration, due to pin misalignment, the pin should be inserted into the block as far as possible (Fig. 10). For the universal joint configuration it is required that $L_p \leq 0.5\ L$. For the special case of the ball-pin universal joint, if the axially transmitted forces are negligible then:

$$L_p \simeq 0.47^*(L - 2R_p) \tag{13}$$

(*2*) In addition, from the standpoint of creating a practical design (Fig. 10), we have:

$$W \simeq L \text{ and } H_1 \simeq 0.5^*L \tag{14}$$

Based on the results acquired from experimental stress analysis for the determination of stress concentration factors [18], the fatigue constraints have been formulated in the following manner:

Design of the Yoke [refer to Figs. 11(*a*) and 11(*b*)]. Since the load distribution acting on the poles of the ball joints are relatively small, and in an effort to decrease the degree of manufacturing difficulty, α, the angle defining the spherical contact area at the ball-yoke connection, is required to be $\leq$ 50 deg, as shown in Fig. 10. Furthermore, the stress concentration at the ball-yoke connection is assumed to approximate that of the cylinder pin-yoke connection. In a worst case analysis, an equivalent cylindrical joint with radius R_b is chosen. The bending fatigue due to the reaction forces may be expressed as:

$$F_b = \max[\max(F_{i2}{}^*\cos\lambda_1),\ \max(F_{i3}{}^*\cos\lambda_2)] \tag{15}$$

$$(\sigma_b)_{max} \geq 12^*K_b{}^*F_b{}^*H_1{}^*R_{ec}/(W - 2R_{ec})^3 t \tag{16}$$[1]

where the stress concentration factor, $K_b = 2.5$, in bending is given by [23]. The yielding fatigue due to the reaction forces may be expressed as:

$$F_y = \max[\max(F_{i2}{}^*\sin\lambda_1),\ \max(F_{i3}{}^*\sin\lambda_2)] \tag{17}$$

By applying a least-squares curve fit to the experimental stress concentration factor data [18] with $\eta = 2^*R_p/W$, yields the following equation:

$$K_y = 7.778 - 18.6\ \eta + 23.26\ \eta^2 - 15.6\ \eta^3 \tag{18}$$

$$(\sigma_y)_{max} \geq K_f{}^*F_y/(W - 2R_{ec})t \tag{19}$$

Assuming that the surface of the ball joint is ideally lubricated, only normal stresses may be transferred across its contact surface. On the boundary of the ball joint there is a sinusoidal stress distribution [16]. With the maximum normal stress denoted by $(\sigma_{rs})_{max}$, force equilibrium can be expressed as:

$$\int_{-\pi/2}^{\pi/2}\int_{-\alpha}^{\alpha} (\sigma_{rs})_{max}\cos^2\phi\cos^2\psi R_b d\phi^* R_b d\psi = F_h \tag{20}$$

where $F_h = \max\ (F_{i2})$.

[1]Actually, the upper surface of the yoke is not flat. This point will be discussed in the following section.

Referring to the geometry shown in Fig. 10, the spherical contact angle, α, for all four ball joints is governed by the following equation.

$$\alpha = \sin^{-1}(t/2R_b) \tag{21}$$

Integrating equation (20) yields:

$$(\sigma_{rs})_{max} = 2F_h/\pi R_b{}^2(\alpha - \sin 2\alpha/2) \tag{22}$$

The surface fatigue constraint requires that:

$$(\sigma_s)_{max} \geq (\sigma_{rs})_{max} \tag{23}$$

Design of the Block [refer to Fig. 11(*c*)]. Assuming the contact surfaces to be ideally lubricated, the normal stress distribution acting on the cylindrical contact surfaces of the pin and block can be described by a sinusoidal function. The corresponding peak stress may be expressed as:

$$P = \max(F_{i2})/L_p \tag{24}$$

where P denotes the load per unit length of the cylindrical pin.

The maximum normal stress is denoted by $(\sigma_{rc})_{max}$. Integrating this stress over the cylindrical contact area between the pin and block yields the load per unit length of the cylindrical pin as follows:

$$\int_{-\pi/2}^{\pi/2} (\sigma_{rc})_{max}\cos^2\phi^* R_d d\phi = P \tag{25}$$

and,

$$(\sigma_{rc})_{max} = 2P/\pi R_p \tag{26}$$

The surface contact fatigue constraint for the floating block may be expressed as:

$$(\sigma_s)_{max} \geq (\sigma_{rc})_{max} = 2P/\pi R_p \tag{27}$$

Since the length of the floating block is much larger than the thickness of the yoke, the constraint corresponding to bending fatigue of the floating block will not be active during the optimization process. Thus, it may be neglected and subsequently checked against the final result.

Design of the Pin [refer to Fig. 11(*d*)]. Bending fatigue due to the applied force may be expressed as:
(The stress concentration factor in bending, K_b, is assumed equal to 2.3 [18]).

$$M_b = F_h{}^*(t/2 + d) \tag{28}$$

$$(\sigma_b)_{max} \geq 32^*2.3^*M_b/\pi R_p{}^2 \tag{29}$$

Geometrical Constraints. In order to prevent the yokes from colliding with each other it is required that:

$$H_2 \geq R + t/2 \tag{30}$$

or, for an optimal design,

$$H_2 = (R + t/2) \tag{31}$$

Furthermore, to prevent yoke-block collision (which depends on the level of the input torque and the amount of resulting deformation), the distance d, between the yoke and block, should be increased in proportion to the magnitude of the input torque. Based on these factors, the distance d has been expressed in terms of the yoke thickness as:

$$d = t/10 \tag{32}$$

Additionally, there are still some important dynamic design considerations, such as inertia induced forces. By adjusting the mass distribution of the universal joint, an improvement of 2.3 percent to 3 percent (rocking torque and internal force reduction) over the original design may be expected [7].

The Application of Numerical Nonlinear Optimization Techniques

Numerical optimization [27] provides a systematic, rational,

and directed approach to design decision-making, where previously heavy reliance was placed on the experience and intuition of the designer in achieving an improved design. Due to complexities involved in the implementation of NLP algorithms for engineering design, several researchers have undertaken performance analyses [12, 23, 24] the purpose being to determine correlations among a set of design problem types, numerical optimization methods, and the corresponding results. It is anticipated that the novice user, having been exposed to these studies, would develop a better understanding of the capabilities of existing optimization algorithms, and would know how to utilize them without the need to carry out exhaustive studies on his own for testing, tuning, and learning. While in concept this appears to be a rational approach to ascertain the capabilities of a particular algorithm for a specific problem, in reality, Himmelblau [8] states that "*a guarantee of convergence for an algorithm for special cases may offer little insight as regards satisfactory strategies for more complex problems.*" We believe that more general NLP algorithm evaluation schemes are required.

Method Switching Strategies in Nonlinear Optimization

Existing algorithms for nonlinear programming which have been surveyed [15, 33] may converge to local optima which are not necessarily global optima. Many techniques for locating global optima, aside from knowing which method is the best first method, have yet to be uncovered. Method switching strategies are based, by analogy, on a *game of golf type of strategy* (sequential application of different NLP algorithms) rather than on the use of a one step optimization scheme. This method switching procedure is designed to be one level higher than the so called optimization strategy level [30, 31] (monitors the numerical optimization process) and sequentially selects suitable numerical method combinations in accordance with local design data [9].

According to the schematic representation depicted in Fig. 12, the first design starting point, $P1$, lies in an infeasible design region and is far away from the globally optimal point. A temporary goal may be expressed as "move the design into the feasible region as soon as possible" to increase the design efficiency. When the design "converges" at a local optimum, $P2$, current NLP methods fail to move away from this point. In accordance with the local information found in the vicinity of $P2$, the method switching manager pins down another temporary goal which may be stated as "find a feasible design with a smaller objective value." Method switching terminates when the convergence criteria have been satisfied. This is usually based on (*1*) a cpu time consumption limitation, (*2*) the number of algorithm iterations, or (*3*) relative or absolute difference between successive values of the objective function. Figure 13 depicts the flow of control utilized in the process of NLP method switching for the optimum geometric design of the universal joint. A more detailed description of this process is provided in the following section.

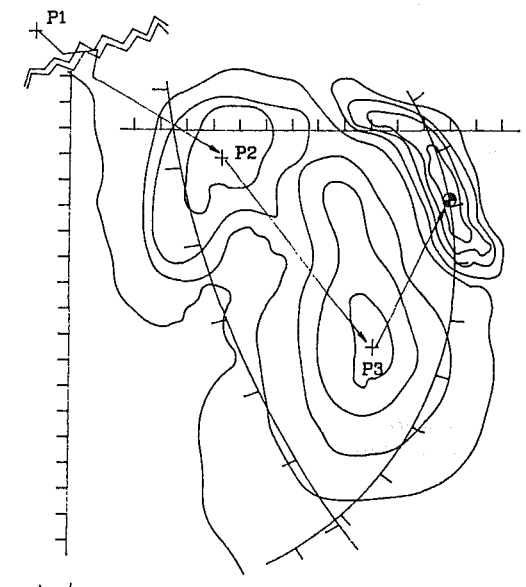

Fig. 12 An example which demonstrates that local design information changes for different design starting points

Numerical Optimization Processing and Results

In this study, the minimum size ball-pin universal joint design is sought based on the parameterized dimensions shown in Fig. 10. The design objective function, denoted as *Obj*, is linear for this problem, and can be expressed in the form:

$$Obj = L + 2(t + d) \tag{34}$$

By making reference to Fig. 10, this design objective can be easily interpreted as the minimization of the shaft diameter for the universal joint.

Initially, there was nothing known about the parameter values corresponding to optimality for this constrained nonlinear programming problem aside from the fact that the constraint

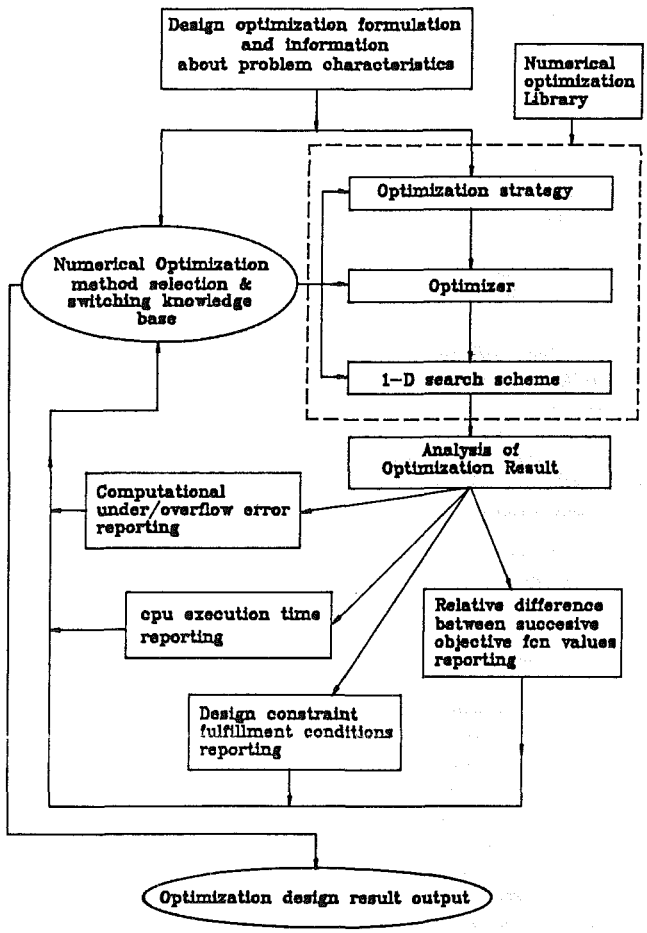

Fig. 13 Flow control for method switching in numerical optimization

functions are highly nonlinear but differentiable between their lower and upper bounds. In addition, the problem size is relatively small, permitting the program to be run on an IBM PC/AT microcomputer.

The following example demonstrates how NLP method switching can be utilized for detailed numerical design optimization. Optimization processing was initiated using the following input and design variable values. Input torque = 100 N-m, Universal joint misalignment angle = 15 deg, Young's Modulus (steel) = 207 GPa, surface yielding stress, $(\sigma_s)_{max}$ = 345 MPa, and tensile fatigue stress, $(\sigma_f)_{max}$ = 345 MPa. The initial design parameter starting values provided are Pin radius (R_p) = 5.0 cm, Block length (L) = 25.4 cm, Yoke thickness (t) = 7.5 cm. The Initial objective function yields a value of the Shaft diameter = Obj (R_p = 5.0, L = 25.4, t = 7.5) = 41.9 cm.

Optimization Run Number One

Optimization history observation:

Since there have been no prior optimization runs, there is no historical information available.

Characteristics of the design optimization problem formulation:

(*1*) The design problem is new and therefore, no existing design dimensions can be referred to. In other words, the initial design parameter guess may be very distant from the optimal design parameter dimensions.
(*2*) The design objective function is linear, while the constraint functions are highly nonlinear within their lower and upper bounds.
(*3*) The design problem size is relatively small, containing only three design variables (R_p, L, t) and five design constraints [equations (16), (19), (23), (27), and (29)].
(*4*) The initial design guess must lie within the feasible design region, since there are no currently active design constraints.

Selection of a nonlinear programming method:

An initial nonlinear programming method was selected in accordance with the design objective and constraint functions characteristics as follows:

Sequential unconstrained minimization (SUMT) was chosen using the quadratic extended interior penalty function method strategy. The Broyden-Fletcher-Goldfarb-Shanno (BFGS) variable metric method was selected for the optimizer for unconstrained minimization. The minimum of the resulting unconstrained function was found using a combination of one-dimensional search algorithms that include the Golden Section method to rapidly establish bounds on the minimum, followed by polynomial interpolation to accurately estimate through interpolation the minimum value of the function over the bounded interval.

Reasons for the selection of the interior penalty function method include:

(*1*) When no information concerning values for the optimum design variables (dimensions) are known a priori, penalty function methods tend to be especially well suited for an optimization search which may potentially require lengthy search distances.
(*2*) For highly nonlinear constraint functions, the reduced gradient method (GRG) and sequential linear programming (SLP) tend to be less robust.
(*3*) Penalty function methods tend to be less efficient than other nonlinear programming methods in the case of large scale design problems. However, the current design problem is of relatively small scale.
(*4*) For the case where the initial starting point for the design lies within the feasible region, an interior penalty function method tends to perform better than an exterior penalty function method.

Upon completion of the first run, the objective function yields a value of:

$$Obj(R_p = .87,\ L = 4.24,\ t = .46) = 5.352 \text{ cm}.$$

Optimization Run Number Two

Optimization history observation:

The result of the first optimization run resulted in a reduction in the design objective function value by a factor of 7.82, with no violations of the design constraints.

Characteristics of the design objective function:

Since no constraints were violated, the characteristics remain the same as in the first run except for the first one (i.e., information concerning the optimal design dimensions are now known). This information was nonexistent during the first run.

Selection of a nonlinear programming method:

A nonlinear programming method is now selected in accordance with the characteristics of the design objective function and the current optimization historical information provided from the previous run:

The performance of the penalty function optimization method is quite good in this design case. However, since the application of the same method combination (i.e., strategy, optimizer and 1-D search scheme) will yield very nearly the same optimum result, (typically only slightly changed), a different selection is made for a one dimensional search scheme in order to find bounds on the unconstrained objective function. Finally, polynomial interpolation was used as the one dimensional search scheme.

Upon completion of the second run, the objective function yields a value of:

$$Obj(R_p = .47,\ L = 2.6,\ t = .23) = 3.106 \text{ cm}.$$

Optimization Run Number Three

Optimization history observation:

The optimization result obtained from the second run reduced the objective function value by a factor of 1.7, without violating any of the design constraints.

Design objective function characteristics:

Since none of the constraints are violated, the characteristics remain the same as in the second run.

Selection of a nonlinear programming method:

A nonlinear programming method is selected in accordance with the design objective function characteristics and the optimization history acquired from the previous run:

(*1*) Penalty function optimization method combinations have been used both in the first and second optimization runs, and the improvement in the result tends to be limited, as seen by the decrease in the rate of improvement of the result (from a factor of 7.82 in run one to a factor of 1.7 in run two).
(*2*) Since the design objective function (shaft diameter) has been decreased by about thirteen fold, the optimization problem has become a tightly constrained problem.
(*3*) The SLP (sequential linear programming) method tends to exhibit better performance than other methods in tightly constrained design problems, and it is therefore chosen for this run.

The result of numerical optimization processing after run number three:

Input Torque, T_{in}	: 100	N-m
Misalignment angle, (β)	: 0.2618	rad
Universal joint shaft diameter, (Obj)	: 2.913	cm
Edge length of the floating block, (L)	: 2.383	cm
Thickness of the yoke, (t)	: 0.241	cm

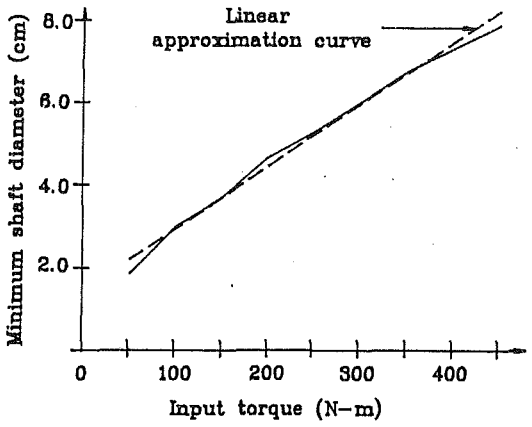

Fig. 14(*a*) Minimum shaft diameter versus input torque

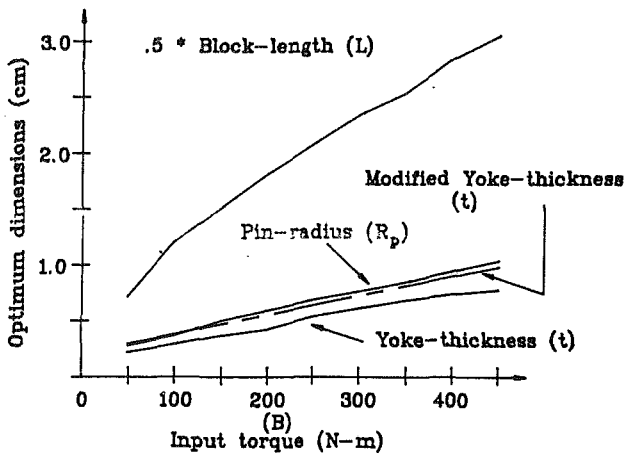

Fig. 14(*b*) Optimum dimensioning of ball-pin type universal joint

The minimum size of the universal joint shaft versus input torque along with the corresponding optimal universal joint dimensions are shown in Figs. 14(*a*) and 14(*b*) [a linear least squares approximation of the result is shown with a dotted line in Fig. 14(*a*)].

Minimum shaft diameter (cm)

$$= 2.2 \text{ (cm)} + .015 \text{ (cm/N-m)}^*\text{(input torque (N-m)} - 500 \text{ (N-m))} \quad (35)$$

The optimal dimensions can also be determined by applying a least squares approximation to the result shown in Fig. 14(*b*). The magnitude of the slopes (rate of increase of dimension with input torque), in order from the highest to the lowest are the floating block length (L), radius of the pins (R_p) and thickness of the yokes (t). Based on these results it can be seen that when the input torque increases, the surface contact constraint, as described by equation (15), becomes less active, whereas bending fatigue of the pin tends to become dominant in the design optimization. However, in the actual physical situation, when the assumption of ideal lubrication does not hold, the shear forces between the pin and the yoke could cause the yoke to twist. Therefore, enlargement of the yoke thickness and yoke thickness slope has been made in Fig. 14(*b*).

Conclusion:

The systematic hybrid optimization scheme introduced herein has been shown to produce mechanism designs which are free of redundant constraints and which possess optimum geometric dimensions. The ramification of the removal of constraint redundancy provides longer-lived and more reliable mechanical devices. In applying this approach to the design of a universal joint several important design improvements were experienced that include (*1*) increased contact area of the pin-yoke connection resulting in decreased contact stress concentration, (*2*) elimination of the reaction forces acting on the input-output shaft bearings, (*3*) isolation of vibration and noise between the input and output shafts and (*4*) elimination of the design unknowns with a subsequent increase in design durability and longevity.

Glossary of Terminology

Global optimum—An optimum design in which the entire feasible region has been searched in order to determine the "best" of all local optima.

Harmful mobility—Unwanted, extra degrees-of-freedom which affect the determinability of the motion of a mechanism and cause the mechanism to fail to operate, possibly in an unexpected manner.

Heuristic rules—Rules of thumb created by a domain expert based on his experience for solving difficult, domain specific, problems.

Independent loops—Independent closed circuits in a mechanism.

Knowledge base—A collection of knowledge, typically in the form of facts and rules, about a specific domain, to be used for decision making.

Local optimum—An optimum design in which only some subset of the feasible region has been searched in order to achieve the optimum. With a local optimum no improvement in the objective function value is possible in the neighborhood, although large excursions may find improved results.

Metacell—A group of design equations for a specific mechanical component which are well organized and have been translated into an expert system programming language.

Optimization strategy—The highest of three levels in a systematic approach to applying numerical optimization to design problems. It converts a constrained optimization problem into an unconstrained optimization problem.

Optimizer—The second of three levels in a systematic approach to applying numerical optimization to design problems. It chooses a one-dimensional search direction.

One-dimensional search technique—The last of three levels in a systematic approach to applying numerical optimization to design problems. It locates the minimum of an unconstrained function using interpolation or some other method (Golden section).

Point-and-surface pair—A kinematic pair possessing five degrees-of-freedom and represented as a point force applied to a surface.

Rational mechanism design—the design of mechanisms in accordance with the concept of elimination of redundant constraints.

Game of golf analogy—The reason for method switching is in accordance with the local geographical design information at the numer-

ical optimum, and is analogous to the reason for selecting an appropriate golf club, in the game of golf, to strike the ball.

Blackboard architecture—A module in a program in which all intermediate messages and results concerning action taken within the program are displayed to the user and stored in a common area, called a blackboard.

Redundant constraints—An indeterminant constraint whose elimination would not increase the mobility (number of degrees-of-freedom) of a mechanism. It represents a redundant internal reaction force or moment having the potential to increase wear and deformation due to misalignment of the links in the mechanism.

Robust higher kinematic pair—A higher kinematic pair constructed by combining lower pairs in order to achieve a pair with greater surface contact and therefore greater load carrying capability with reduced awkwardness than that possible with regular higher pairs alone.

Systolic cell—A standardized design metacell containing a regular program interface with the capability of communicating with other metacells.

Acknowledgments

The authors gratefully acknowledge the research support provided by the United States Army Research Office under grant DAAL03-86-K-0071 and by the United States Army Research Office-Department of Defense University Instrumentation Program under grant DAAL03-86-6-0116. In addition, the support provided by the IBM Corporation through the IBM Manufacturing Fellowship Program and by the Carnegie Group for the use of the Knowledge Craft expert system development environment are also gratefully acknowledged. Additionally, the authors would like to thank Professor Ferdinand Freudenstein for his advice, guidance,and encouragement.

References

1 Buchsbaum, F., and Freudenstein, F., *Design and Application of Small Standardized Components*, Thorton, P. J., ed., Stock Drive Products Co., 1983.

2 Chieng, W. H., and Hoeltzel, D. A., "An Interactive Hybrid (Symbolic-Numeric) System Approach to Near Optimal Design of Mechanical Components," *Engineering with Computers*, Springer-Verlag Publishers, Vol. 2, No. 2, 1987, pp. 111-123.

3 Curtis Universal Joint Manufacturing Co. Catalog, 1986.

4 Dym, C. L., "Expert Systems: New Approaches to Computer-Aided Engineering," *Engineering with Computers*, Springer-Verlag Publishers, Vol. 1, No. 1, 1985, pp. 9-25.

5 Fischer, I. S., and Freudenstein, F., "Internal Force and Moment Transmission in a Cardan Joint with Manufacturing Tolerance," ASME JOURNAL OF MECHANISMS, TRANSMISSIONS, AND AUTOMATION IN DESIGN, 1984, pp. 301-311.

6 Freudenstein, F., and Maki, E. R., "The Creation of Mechanisms According to Kinematic Structure and Function," General Motors Research Report, No. GMR-3073, 1980, p. 378.

7 Gill, G. S., and Freudenstein, F., "Minimization of Inertia-Induced Forces in Spherical Four-Bar Mechanisms, Part I," ASME JOURNAL OF MECHANISMS, TRANSMISSIONS, AND AUTOMATION IN DESIGN, 1983, pp. 471-483.

8 Himmelblau, D., *Applied Nonlinear Programming*, McGraw-Hill Book Co., 1972.

9 Hoeltzel, D. A., and Chieng, W. H., "Statistical Machine Learning for the Cognitive Selection of Nonlinear Programming Algorithms in Engineering Design Optimization, Advances in Design Automation," ASME Pub. No. DE-VOL. 10-1, 1987, pp. 67-74.

10 Kitzmiller, C. T., and Kowalik, J. S., "Coupling Symbolic and Numeric Computing in Knowledge-Based Systems," *AI Magazine*, Vol. 8, No. 2, 1987, pp. 85-90.

11 Lee, D. A., "Estimating Universal Joint Performance Variations," *Machine Design*, 1965, pp. 151-153.

12 Lootsma, F. A., "Performance Evaluation of Nonlinear Optimization Methods via Multi-Criteria Decision Analysis and via Linear Model Analysis," *Nonlinear Optimization 1981*, M. J. D. Powell, ed., Academic Press, NATO Conference Series, 1981, pp. 419-453.

13 Malyshev, A. P., *Analysis and Synthesis of Mechanisms from the Viewpoint of Their Structure*, Izv. Tomsk, Tekh. Inst., 1923, (in Russian).

14 Mazziotti, P. J., "Dynamic Characteristics of Truck Driveline Systems," SAE Paper No. 650189, 1966, pp. 851-887.

15 McCormick, G. P., *Nonlinear programming: Theory, Algorithms, and Applications*, John Wiley & Sons, New York, 1983.

16 McCutchen, C. W., "The Frictional Properties of Animal Joints," *Wear*, Vol. 5, 1962, p. 7

17 Ozol, O. G., "On New Structural Formula," *Izvestiya Vyshikh Uchebnykh Zavendi*, No. 4, 1964, pp. 49-58 (in Russian).

18 Peterson, R. E., *Stress Concentration Factors*, John Wiley & Sons, 1974.

19 Porat, I., "Moment Transmission by a Universal Joint," *Mechanism and Machine Theory*, Pergamon Press, Vol. 15, 1980, pp. 245-254.

20 Reshetov, L. N., "Designing Rational Mechanisms," *Vestnik mashinostroeniya*, No. 5, 1958, pp. 3-10, (in Russian).

21 Reshetov, L. N., and Bukykas, E. Yu., "The Problem of Determining Redundant Constrints in Mechanisms," *Izvestiya Vysshikh Uchebnykh Zavendi*, Engineering Series, No. 3, 1976, pp. 68-70, (in Russian).

22 Reshetov, L., *Self-Aligning Mechanisms*, MIR Publishers, Moscow, 1982, pp. 8-81.

23 Sandgren, E., and Ragsdell, K. M., "The Utility of Nonlinear Programming Algorithms: A Comparative Study, Part I & II," ASME JOURNAL OF MECHANICAL DESIGN, 1980, pp. 540-551.

24 Schittkowski, K., *Nonlinear Programming Codes, Lecture Notes in Economics and Mathematical Systems*, Springer-Verlag, Berlin, 1980.

25 Schweralin, H., "Combating Heat in Universal Joints," *Machine Design*, Vol. 53, No. 17, July, 1981, pp. 83-86.

26 Shamaidenko, N. E., "On Using Kinematic Connections Instead of Kinematic Pairs for the Rational Design of Mechanisms," *Izvestiya Vysshikh Uchebnykh Zavendi*, Engineering Series, No. 6, 1964, pp. 26-31, (in Russian).

27 Siddall, J. N., *Optimal Engineering Design: Principles and Applications*, Marcel-Dekker Pub., Inc., 1982.

28 Soni, A. H., *Mechanism Synthesis and Analysis*, McGraw-Hill Book Co., 1974, p. 2.

29 Universal Joint and Driveshaft Design Manual: SAE Advances in Engineering Series No. 7, Published by the Society of Automotive Engineers, 1979.

30 Vanderplaats, G. N., *Numerical Optimization Techniques for Engineering Design: with Applications*, McGraw-Hill Book Co., 1984.

31 Vanderplaats, G. N., ADS—Fortran Program for Automated Design Synthesis, NASA Contract Report 172460, 1984.

32 Whitehead, T. N., *The Design and Use of Instruments and Accurate Mechanisms*, Macmillan Book Co., 1934.

33 Wilde, D., *Globally Optimal Design*, John Wiley & Sons, New York, 1978.

34 Yang, A. T., "Static Torque and Force Analysis of a Spherical Four Bar Mechanism," ASME *Journal of Engineering for Industry*, Vol. 87, 1965, pp. 221-227.

APPENDIX

The Enumeration of Series Kinematic Connections

A brief overview of the process of generating series kinematic connections, that is, the connection in series of lower kinematic pairs to obtain higher pairs for the purpose of obtaining joints which are robust and free of redundant constraints and harmful mobilities, will be presented. The little known work of L. Reshetov et al. [11, 18], N. E. Shamaidenko [19], and Reshetov and Bukykas [20], from the relatively obscure Soviet engineering literature, has been adapted as the basis for this discussion.

N. E. Shamaidenko [19] has determined that with pairs connected in series mobilities add, thereby enabling the synthesis of kinematic connections having two, three, four, and five degrees of freedom from combinations of lower pairs having one, two, and three degrees of freedom. L. Reshetov and E. Yu. Bukykas [20] have elaborated on this idea and found that with kinematic pairs connected serially, there remain only the constraints which are commonly shared among those pairs. This is due to the fact that when a pair has a mobility corresponding to a constraint in an adjacent, serially connected pair, the constraint cannot be transmitted (propagated) through the connection. This applies only to cases where

Table A1 Serially connected kinematic pairs. (Adapted from L. Reshetov, 1982)

Class \ Type	(a)	(b)	(c)	(d)	(e)	(f)
I	5=3+2 Q_z 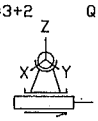	5=3+1+1 Q_z 	5=2+2+1 Q_z 	5=2+1+1+1 Q_z 	5=1+1+1+1+1 Q_z 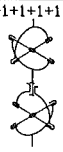	5=1+1+1+1+1 M_z 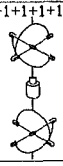 ⊗
II	4=3+1 Q_x Q_z 	4=2+1+1 Q_x Q_z 	4=1+1+1+1 Q_z M_z 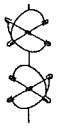 ⊗	4=2+2 Q_z M_z  ⊗	4=1+1+2 Q_z M_y 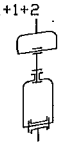	4=1+3 M_x M_y 
III	3=1+1+1 Q_x Q_y Q_z 	3=1+1+1 Q_x Q_y M_z 	3=1+2 Q_x Q_z M_z 	3=1+2 Q_y M_y M_z 	3=1+1+1 Q_z M_x M_z 	3=1+1+1 M_x M_y M_z  ⊗
IV	2=1+1 Q_x Q_y Q_z M_z 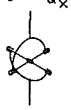	2=1+1 Q_y Q_z M_x M_z 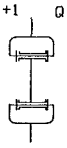 ⊗	2=1+1 Q_x Q_y M_y M_z  ⊗	2=1+1 Q_x Q_z M_x M_z 	2=1+1 Q_z M_x M_y M_z  ⊗	Local Coordinate System 

the lines of action (translation) or axes of rotation of the pairs coincide. When this is not the case, the situation can become quite complicated since translational and angular mobilities become interchanged.

L. Reshetov [11] has compiled a table of series kinematic connections with constraints ranging from one through five, and has assigned a classification scheme whereby a pair having i constraints is referred to as a Class i pair. For example, a pair having 3 constraints is called a Class III pair. Also, each class has been further subdivided according to type (a through f). A modified version of Reshetov's table of series kinematic connections, consistent with the notation used in Table 2, has been included for clarification of the concepts discussed above. Each entry in Table A1 includes (*1*) a skeleton diagram of the kinematic connection, (*2*) the assignment of the mobilities (degrees-of-freedom) in that pair (total degrees-of-freedom = rotational dof + translational dof) along with the force, Q_i, or moment, M_i, transmitted by the joint and the corresponding axis along which the force or moment acts and (3) a symbol, ⊗, indicating, where applicable, that there is no single theoretical higher pair corresponding to this kinematic connection.